ISSN 0036-0236, Russian Journal of Inorganic Chemistry, 2012, Vol. 57, No. 6, pp. 769–776. © Pleiades Publishing, Ltd., 2012.
Original Russian Text © A.I. Bulavchenko, M.G. Demidova, T.Yu. Podlipskaya, V.V. Tatarchuk, I.A. Druzhinina, A.V. Alekseev, V.A. Logvinenko, V.A. Drebushchak, 2012, published in Zhurnal Neorganicheskoi Khimii, 2012, Vol. 57, No. 6, pp. 839–846.

SYNTHESIS AND PROPERTIES OF INORGANIC COMPOUNDS

Microemulstion Synthesis of Powders of Water-Soluble Energy-Saturated Salts

A. I. Bulavchenko, M. G. Demidova, T. Yu. Podlipskaya, V. V. Tatarchuk, I. A. Druzhinina, A. V. Alekseev, V. A. Logvinenko, and V. A. Drebushchak

Nikolaev Institute of Inorganic Chemistry, Siberian Branch, Russian Academy of Sciences, pr. Akademika Lavrent'eva 3, Novosibirsk, 630090 Russia

Received March 15, 2011

Abstract—The feasibility of preparing energy-saturated salts (NH_4NO_3, KNO_3, and $NaBH_4$) in powders with various particle sizes in microemulsion systems based on oxyethylated surfactant Tergitol NP-4 has been demonstrated. Powders were isolated by destroying microemulsions with acetone. The regions of micellar synthesis have been determined depending on the solubilization capacities and concentrations of the reagents and salts at a fixed Tergitol NP-4 concentration (0.25 mol/L). The morphologies and particle sizes of the thus-prepared salt powders were characterized by scanning electron microscopy (SEM), X-ray powder diffraction, differential scanning calorimetry (DSC), differential thermal analysis (DTA), and thermogravimetry; the hydrodynamic radii of microemulsions were characterized by photon-correlation spectroscopy.

DOI: 10.1134/S003602361206006X

Microemulsion (micellar) synthesis is a popular method and is widely used for preparing nanoparticles of metals [1], oxides [2], and sparingly soluble salts [3, 4]. The advantages of this method include: (1) the ease of synthesis; (2) a narrow particle-size distribution function of the product; (3) a feasibility of preparing particles of complex composition, multilayered, hybrid, and other types of particles [5]; and (4) a good knowledge of the micellar and microemulsion structure. Unfortunately, there only few studies directed to the preparation of nanoparticles of water-soluble salts by the microemulsion method. For example, $Co(NO_3)_2$, $CaCl_2$, Na_2HPO_4, and $Cu(NO_3)_2$ nanoparticles have been prepared in a solid-phase concentrate in an AOT matrix (sodium di(2-ethylhexyl)sulfosuccinate) via distilling off the solvent (heptane) and water [6, 7].

Meanwhile, studies of microemulsion synthesis as applied to prepare powders and liquid hydrophobic concentrates of nanoparticles of water-soluble energy-intensive salts seem to be very promising for both science and application. For example, reverse emulsions of supersaturated ammonium nitrate solutions [8, 9] in diesel fuel have almost substituted for TNT-containing industrial explosives [10–13].

Our goal here was to study the possibility of preparing powders of water-soluble salts in reverse microemulsions of oxyethylated surfactant Tergitol NP-4.

EXPERIMENTAL

Reagents

The micelle-forming surfactant used was oxyethylated nonylphenol with an average oxyethylation number of four, namely, Tergitol NP-4 (from Dow Chemical). A micellar solution contained 0.25 mol/L Tergitol NP-4 in *n*-decane. The organic solvents used were pure grade *n*-decane and *N*,*N*-dimethylformamide (DMF) and high purity grade heptane and acetone. The initial reagents used were concentrated nitric acid (high purity grade, 16.2 mol/L), concentrated aqueous ammonia (high purity grade, 10.8 mol/L), KOH, and $NaBH_4$ (both of pure grade), NH_4NO_3 (pure for analysis grade), and KNO_3 (chemically pure grade).

Structural Study of Microemulsions and Powders

The limiting solubilization capacity V_s/V_o (the volume ratio of an aqueous solubilizate solution to a solubilizate-containing micellar solution) of a microemulsion system with respect to aqueous solutions of reagents and salts was determined by serial injections of small volumes of the aqueous phase. The cloud point was detected visually and spectrophotometrically by an abrupt increase in the absorbance of the solution. Measurements were carried out on a Shimadzu 1700 spectrophotometer using quartz cells (l = 1 cm); the reference solution was a "dry" micellar solution.

Microemulsions with initial reagents were structurally studied by photon-correlation spectroscopy and

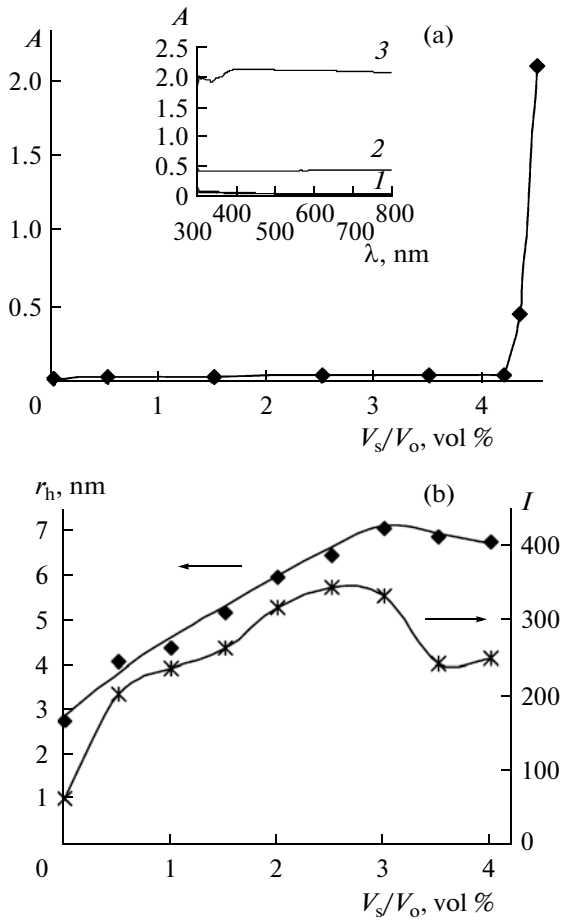

Fig. 1. (a) Absorbance A at $\lambda = 800$ nm and (b) hydrodynamic radius r_h and light scattering intensity I vs solubilization capacity of the micellar solution V_s/V_o for the solubilization of water. In the inset: absorption spectra of micellar solutions with different water contents: (*1*) 4.2, (*2*) 4.3, and (*3*) 4.5 vol %.

static light scattering. Aqueous electrolyte solutions were introduced into micellar solutions of Tergitol NP-4 by injection. All microemulsions obtained in this manner and the initial "dry" micellar solution were dedusted by five- to tenfold cyclic filtering through no. 5 glass Schott filter (with a pore size of 5.1 μm) in a closed box. Strongly opalescent and clouded systems with large-size particles were not dedusted. Measurements were carried out at a 90° angle in quartz cells ($l = 1$ cm) on a 90Plus Brookhaven Inst. spectrometer. A Lasermax solid-state laser had a power of 35 mW; the wavelength was 658 nm; scattered photons were accumulated by a high-sensitivity APD detector (Perkin-Elmer). The z-average hydrodynamic radius [14] was calculated as the average of 10 measurements using the Stokes–Einstein relationship for spherical particles [15]. The photon accumulation time was 10 s. Temperature was maintained with an accuracy of 0.1 K; the measurement error in hydrodynamic radius did not exceed 5%.

The scattered light intensity was determined at a 90° angle using a 90Plus spectrometer as the count rate (the scattered photon number per millisecond).

The morphology and particle size of ultrafine powders were studied with a JEOL JSM-6460LV scanning electron microscope on a graphite substrate.

X-ray powder diffraction studies of polycrystalline samples were carried out on a DRON-3M automated powder diffractometer ($R = 192$ mm, CuK_α radiation, Ni filter, a scintillation detector with amplitude discrimination, 2.5° Soller slits on the primary and reflected beams) in a 2θ range of 5°–70° with scan steps of 0.03° and exposure time per point of 1 s.

In some cases (for small samples or strong preferred orientation of crystallites), patterns were recorded in Debye–Scherrer geometry on a Bruker X8 APEX single-crystal diffractometer (MoK_α radiation, graphite monochromator) as described in [16]. Diffraction patterns were recorded with a CCD area detector which was positioned normal to the primary beam (detector resolution: 1024 × 1024 pixels; sample-to-detector distance: 50 mm; exposure time: 15 min).

X-ray phase analysis was carried out in an automated mode with reference to the PDF-2 power data file [17]. Crystallite sizes were derived from the integrated widths of single diffraction lines using the Scherrer relationship and with a correction applied for instrumental line broadening (the reference was corundum).

Calorimetric measurements were carried out on a DSC-204 Netzsch differential scanning calorimeter using standard (40-μL) aluminum crucibles in a dry argon flow (10 mL/min) at a heating rate of 6 K/min. Ammonium nitrate sample sizes were 12.50 mg (for the commercially available product) and 5.07 mg (for the synthesized samples).

TGA and DTA curves were obtained with a Netzsch TG 209 F1 calorimeter (sample sizes: 1 to 10 mg; heating rate: 9.6 K/min).

Preparation of Powders

Microemulsions of NH_4NO_3 and KNO_3 aqueous solutions were prepared in two routes: (1) from the reagents by a neutralization reaction and (2) from commercially available salts.

According to the first route, to a microemulsion with a solubilized ammonia solution, nitric acid was additionally injected. In order to prepare HNO_3, the order in which reagents (HNO_3 and KOH) were added was opposite. The reagent ratio was stoichiometric, or a multiple excess of one reagent was created. According to the second route, an aqueous solution of a salt (NH_4NO_3 or KNO_3) was solubilized into micelles.

Powders were isolated from microemulsions by destroying the microemulsions by acetone. The particular conditions for preparing microemulsions and for isolating ultrafine salt powders from them were as

follows (for the samples that were characterized by scanning electron microscopy).

First synthesis route. Concentrated aqueous ammonia was introduced into a micellar solution by injection solubilization to a concentration of up to 1.5 vol %; into the resulting solution, concentrated nitric acid was then solubilized so that the ratio $NH_3 : HNO_3 = 1.5 : 1$ was held.

Second synthesis route. In order to obtain precursor microemulsions, an aqueous solution of 2 M KNO_3 was injected in two aliquots into the micellar solution under stirring for 2 and 10 min. The concentration of the solubilized aqueous phase was 2 vol %.

From the microemulsions prepared in this way, NH_4NO_3 and KNO_3 powders were isolated by diluting them with acetone in the volume ratio 1 : 1. The isolated powders were washed with acetone and then three times with heptane; then, they were dried in air and stored in glass weighing bottles inside a desiccator over P_2O_5. Products yields were 35–75%.

A specific situation occurred with $NaBH_4$, which is vigorously decomposed by acids, and hydrolyzes in water and aqueous (even concentrated) ammonia solutions and in aqueous alkalis with concentrations less than 2 mol/L. Of the nonaqueous polar solvents, DMF is one of the best for $NaBH_4$ because of providing solubilities of about 16% and stable solutions [18]; we used it in studying solubilization. Having low solubilization capacities, DMF solutions of borohydride were unsuitable for preparing microemulsions with considerable $NaBH_4$ concentrations. For this reason, ultrafine $NaBH_4$ powders were prepared by means of strongly reducing the polarity of the medium and rapidly crystallizing the salt in the presence of a surfactant in acetone. For this purpose, we mixed equal volumes of the saturated solution of $NaBH_4$ in DMF and a solution of 0.5 M Tergitol NP-4 in acetone; acetone is completely miscible with DMF but does not dissolve borohydride. The resulting suspension was centrifuged; the mother solution was decanted; the precipitate was washed several times with acetone and heptane (also by decantation) and stored under heptane. In order to study solid product samples, the solvent was removed by unforced evaporation at room temperature. The product yield was 80%.

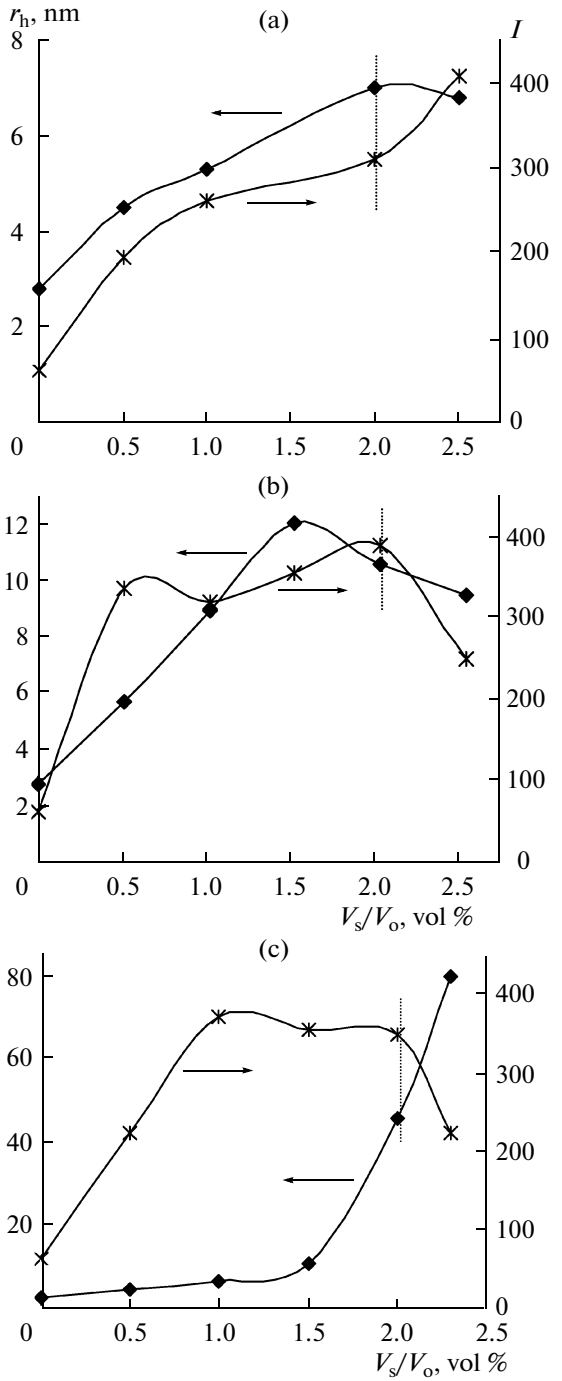

Fig. 2. Light scattering intensity I and hydrodynamic radius r_h vs solubilization capacity of the micellar solution V_s/V_o for the solubilization of (a) 2 M KNO_3, (b) 8 M NH_4NO_3, and (c) 4 M HNO_3. The dotted line marks the limiting solubilization capacity determined spectrophotometrically.

RESULTS AND DISCUSSION

Preparation and Characterization of Precursor Microemulsions for Synthesis

Solubilization was studied both for the initial reagents (acids and bases) and synthesis products (salts). This was necessitated by the following: first, the need to determine the optimal reagent concentrations to provide a maximal product yield; and second, a relationship between the solubilization capacity, on one the hand, and micelle sizes [19] and, accordingly, the resulting particle sizes, on the other. In choosing nonionic oxyethylated surfactant (Tergitol NP-4) and solvent (*n*-decane) to be used in synthesis, we were guided by the greater universality of and tolerance of solutions of nonionic surfactants in saturated hydro-

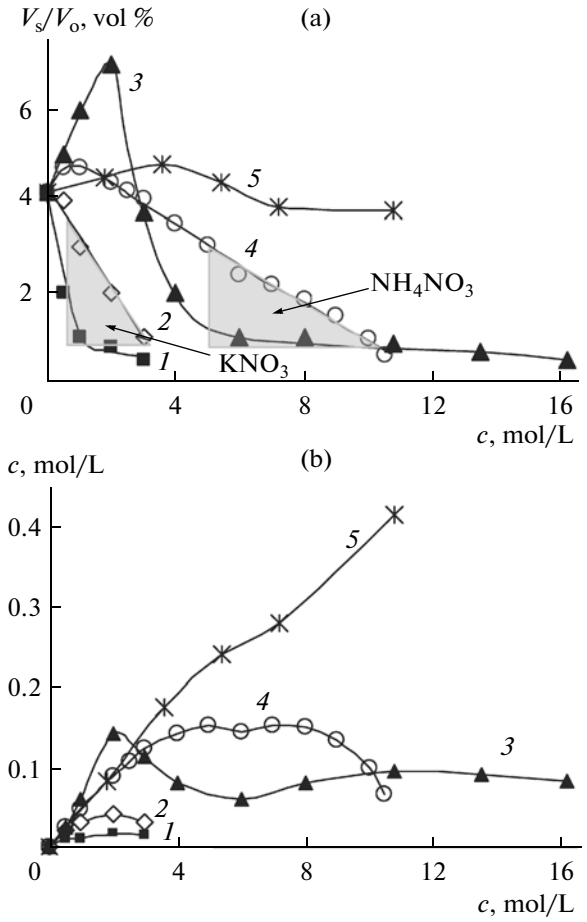

Fig. 3. (a) Solubilization capacity and (b) concentration in the micellar solution of Tergitol NP-4 vs electrolyte concentration in the aqueous pseudo-phase: (*1*) KOH, (*2*) KNO_3, (*3*) HNO_3, (*4*) NH_4NO_3, and (*5*) NH_4OH.

carbons toward electrolytes compared to ionic surfactants [20].

First, we studied the solubilization capacity of a solution of Tergitol NP-4 in decane for pure water, which is the major solubilizer. Figure 1a shows the apparent absorbance (at $\lambda = 800$ nm) with the absorption spectrum (in the inset) as a function of solubilization capacity for water. The cloud point was detected as the strong increase in absorbance of the solution. Similar curves were obtained for all systems under study. Noticeable is good convergence between the spectrophotometric data and the results of visual detection. The hydrodynamic radius and scattered light intensity are shown in Fig. 1b as a function of solubilization capacity for water as the initial base system. Noticeable are weak maxima at 3.0% aqueous pseudophase. For solubilization capacities greater than 4.0%, the hydrodynamic radius abruptly increases at the cloud point to 150 nm (these data are not shown in Fig. 1b).

Composition of the microemulsions and KNO_3 yields (the second synthesis route by the scheme Tergitol NP-4 $\longrightarrow$ HNO_3 $\longrightarrow$ KOH + acetone (1 : 1)) at fixed (nos. 1–4) and variable (nos. 5–7) aqueous pseudo-phase contents

No.	Microemulsion		KNO_3 yield, %
	aqueous pseudo-phase content, vol %	KNO_3 concentration in microemulsion, mol/L	
1	2	0.005	0
2	2	0.01	26
3	2	0.02	45
4	2	0.04	73
5	0.5	0.01	36
6	1	0.02	63
7	2	0.04	73

For solubilization of salt solutions, similar curves were obtained (Figs. 2a, 2b). The curve for nitric acid has a slightly different trend (Fig. 2c). The hydrodynamic radius starts to rapidly increase before reaching the cloud point due to the formation of strongly extended micelles. The curves we obtained agree with those obtained earlier [19, 20]. Noticeable is a poor precision of the results (especially in regard of light scattering intensity) in the vicinity of the cloud point, which is because of the systems being unstable. The visual detection and spectrophotometric determination of the cloud point give more precise results compared to photon correlation spectroscopy and static light scattering. Therefore, these methods were used to determine limiting solubilization capacities (Fig. 3).

The limiting solubilization capacities of micellar solutions upon injection solubilization were shown to decrease, as concentration increases, in the following order: acids > bases ~ salts (Fig. 3a). The least solubilization was noticed for KOH. For HNO_3, the solubilization has a well-defined maximum (7 vol %) for a concentration of 2 mol/L. We had established similar trends for HCl and H_2SO_4 [20]. Noticeable are abnormally high capacities (4–5 vol %) for NH_4NO_3 and NH_4OH; at low concentrations, they are close to the solubilization capacity for acid, and at high concentrations, even exceed it.

The different solubilization characters of the reagents arise from their different natures and the ampholitic properties of Tergitol NP-4. Due to having oxyethyl groups and a hydroxide group, the surfactant has noticeable basic properties (the protonation constant $K_H = 10^{-2}$ to 10^{-3}) [21], and due to the dissociation of the hydroxide group, it behaves as a weak acid ($K_a = 10^{-11}$) [22]. The solubilized compounds are strong electrolytes (salts, nitric acid, and potassium hydroxide), a weak base (ammonia; $K_b = 1.8 \times 10^{-5}$), and a weak cationic acid (NH_4^+; $K_a = 5.5 \times 10^{-10}$) [23]. The other conditions being equal, evidently, the solubilization capacity for a solution of a strong base is lower than for a weak one. The preferred interaction of ammonium ions with the oxyethyl groups of the surfactant (compared to potassium ions) had been shown in [24].

For monitoring the synthesis output, it is necessary to know the overall salt content in the organic phase (Fig. 3b). Once the solubilization capacity and overall salt concentration are known, one can choose both the optimal reagent composition for synthesis and the micelle sizes. In preparing ammonium nitrate by the second route, the same high salt contents can be provided by adding micelles with 3 vol % of 5 M NH_4NO_3 solution or 2 vol % of a 7.5 M solution.

The solubilization of aqueous $NaBH_4$ solutions is accompanied with H_2 evolution because of hydrolysis of the salt. Stable aqueous solutions of $NaBH_4$ were obtained only on the basis of 2 M NaOH. In solutions based on concentrated NH_4OH solutions and 0.1 M NaOH, sodium borohydride slowly decomposes despite of their alkalinity. For solutions of ~3 mol/L $NaBH_4$ in concentrated NH_4OH, the solubilization capacity of Tergitol NP-4 solution was on the order of 1 vol %. This dictated the need for finding alternative solvents for $NaBH_4$. Stable $NaBH_4$ solutions with concentrations of up to 1.6 mol/L were prepared in DMF. The solubilization capacity of a decane solution of Tergitol NP-4 for DMF solutions of $NaBH_4$ was almost independent of borohydride concentration (up to 1.6 mol/L) and was 1.5 vol %, as for DMF,

In this way, microemulsions with different concentrations of the reagents and aqueous pseudo-phase and with different polarities of micellar cores and sizes of polar cores were provided for the synthesis.

Separation of Powders from Microemulsions. Spontaneous separation of salts from microemulsions was not observed during synthesis. Noticeably, the opposite situation is more frequently observed in reduction of metals: it is quite problematic to obtain stable microemulsions with nanoparticles, because coagulation frequently starts during synthesis [25]. The situation with water-soluble salts is more complex: in microemulsions, we have not salt nanoparticles; rather, we have their solutions. Therefore, for separating powders from microemulsions containing aqueous salt solutions, the following is necessary: (1) to obtain nanoparticles by decreasing the polarity of aqueous micellar cores and thereby reducing salt solubilities; (2) to induce coagulation of nanoparticles by destroying micelles; and (3) to retain micellar water in the organic phase in order to keep the separated salt from being dissolved by desolubilized water. For isolating metal nanoparticles in similar cases, polar organic solvents are used [26] where surfactants dissolve better than in saturated hydrocarbons and do not form micelles. As a result, nanoparticles are deprived of the protective surfactant layer, and osmotic repulsion strongly decreases. The potential well depth becomes greater due to the fact that particles can come to small distances to each other and coagulation starts in the system.

Of the polar solvents used to isolate powders, acetone was most efficient with acetone-to-microemulsion phase ratios of at least 1 : 1 (vol/vol). For Tergitol

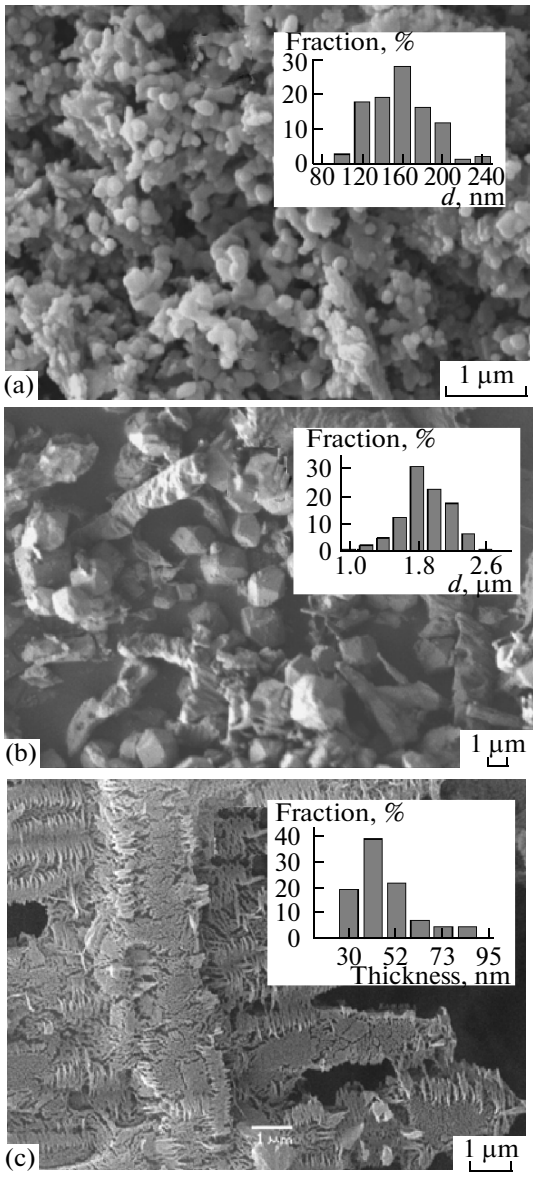

Fig. 4. SEM images and particle-size distribution functions for (a) sodium borohydride, (b) potassium nitrate, and (c) ammonium nitrate powders.

NP-4 microemulsions, ultrafine crystalline powders can be separated only within certain ranges of reagent concentrations (and reagent ratios) and aqueous pseudo-phase contents (the first synthesis route). In preparing ammonium nitrate from HNO_3 and NH_4OH, product separation was observed only when the aqueous pseudo-phase content was 1.3 to 2 vol % (for concentrated reagent solutions) with the stoichiometric reagent ratio and up to a twofold excess of NH_4OH. In preparing KNO_3 by the neutralization reaction, the opposite situation was observed: the salt was isolated only with the stoichiometric reagent ratio or in an excess of HNO_3 (up to a fourfold excess). Salt separation by acetone occurred only when salt con-

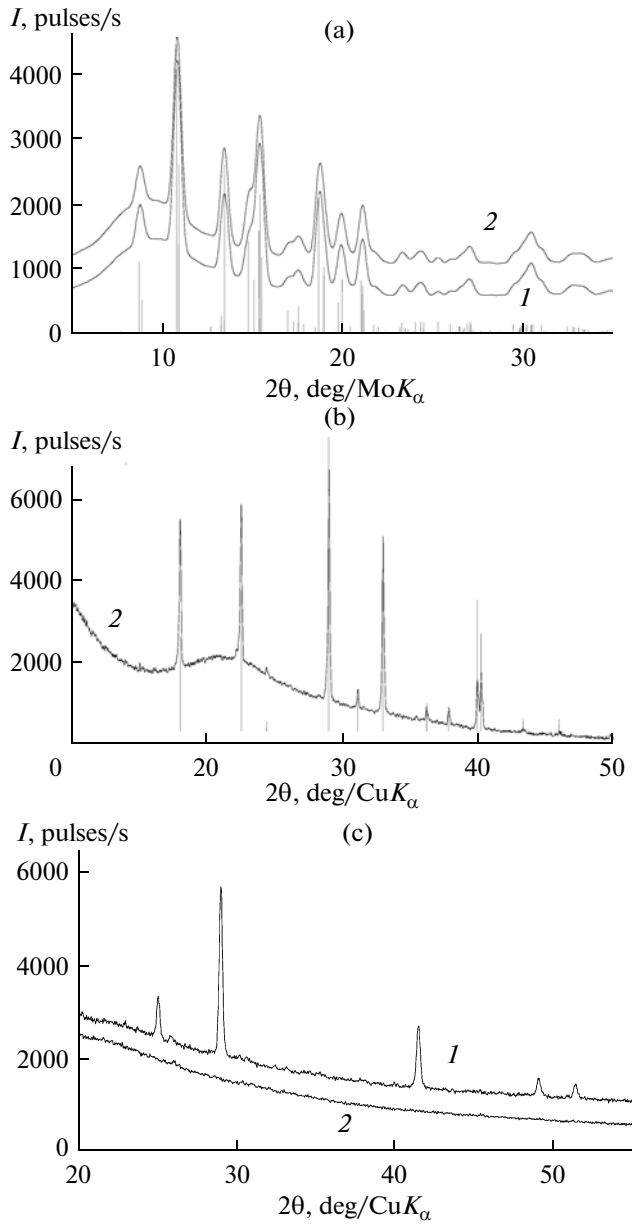

Fig. 5. X-ray diffraction patterns for (a) KNO_3, (b) NH_4NO_3, and (c) KBH_4: (*1*) the initial salts and (*2*) prepared samples. Vertical lines show peak positions for the reference samples of KNO_3 (PDF no. 71-1558), NH_4NO_3 (PDF no. 74-1891), and KBH_4 (PDF no. 74-1891).

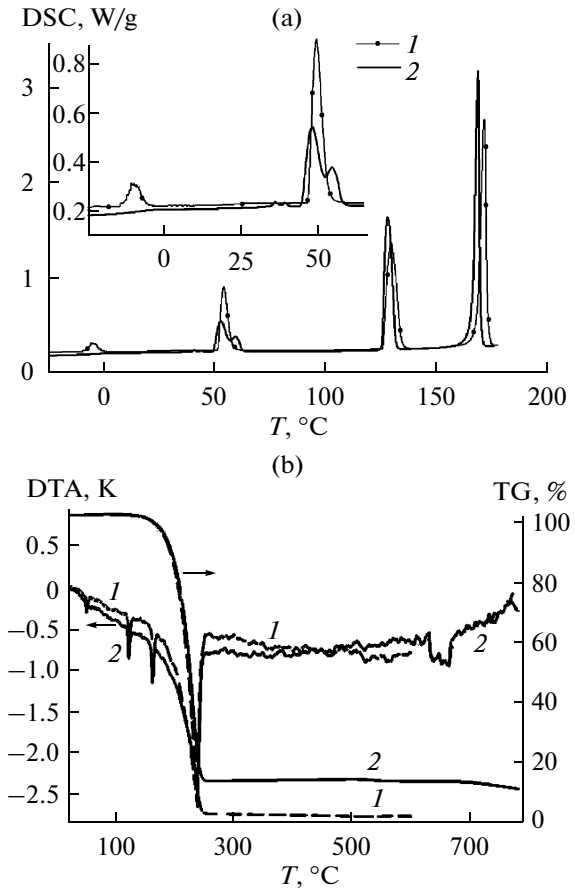

Fig. 6. (a) DSC and (b) DTA and TG data for NH_4NO_3 samples: (*1*) a reference and (*2*) a sample prepared by micellar synthesis. In inset (a): the low-temperature DSC range.

centrations in solubilized solutions were higher than 0.5 mol/L. The acid could enhance the solubility of NH_4NO_3 and suppress the solubility of KNO_3 in the complex multicomponent system water(salt–acid(base))–decane–acetone –Tergitol NP-4.

When ammonium nitrate was separated from the microemulsion obtained by the injection solubilization of NH_4NO_3 (the second synthesis route), a precipitate appeared only when NH_4NO_3 concentrations were higher than 5 mol/L and aqueous pseudo-phase contents were 0.8–3.1 vol %. Potassium nitrate was separated when concentrations were higher than 0.5 mol/L and aqueous pseudo-phase contents were 0.8–4 vol % (the regions for separating NH_4NO_3 and KNO_3 powders are shown in Fig. 3a schematically). Thus, the salt separation regions are bounded from above by the solubilization curve, and from the left and from below, by some minimal concentrations and solubilization capacities as specified above. In order for powders to be separated, it is evidently necessary that both the salt content and water content in the microemulsion be optimal. In moving to the "left" from the aforementioned regions, addition of acetone gives rise to the separation of microemulsions into two liquid phases of comparable volumes (their compositions and structures have not been studied). In moving "down," neither phase separation nor powder isolation occurs.

For KNO_3, it was shown that the salt yield in the separation region is not constant; rather, it is proportional to the salt concentration in the reverse-micellar solution (table). Measurements were carried out with a fixed aqueous pseudo-phase content by varying salt concentration (samples 1–4) or with a fixed salt con-

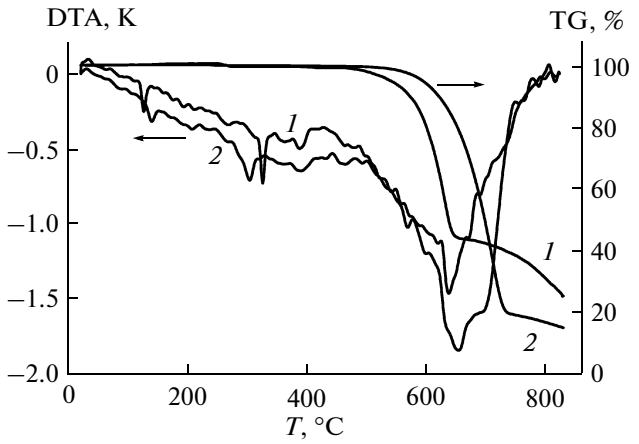

Fig. 7. DTA and TG data for KNO_3 samples: (*1*) a reference and (*2*) a sample prepared by micellar synthesis.

centration in the concentrate by varying aqueous pseudo-phase content (samples 5–7). In the former case, the water content in microemulsions was fixed and in the latter was not. The closeness of values suggests that the water content in the synthesis region is not the decisive factor; rather, the salt concentration in the organic phase is. Although, naturally, the water content should influence the particle size and morphology of the resulting powder.

Characterization of Powders

NH_4NO_3, KNO_3, and $NaBH_4$ powder samples prepared by the routes described in the Experimental section have been characterized by scanning electron microscopy (Fig. 4). Noticeable are different morphologies and particle sizes. For sodium borohydride (Fig. 4a), particle shapes were more close to spherical ones; for potassium nitrate particles (Fig. 4b), faceting was characteristic. The ammonium nitrate powder (Fig. 4c) isolated from microemulsion consisted of thin needles. Needles grow together by their ends to form extended dendrite-like structures that resembled twigs or snowflakes when viewed under small magnifications. Attempts to take higher resolution images and to redisperse sample ultrasonically failed because of the particles melting (decomposing) under the electron beam. Transmission electron microscopy failed for the same reasons. The particle-size distribution diagrams of the salts displayed in Fig. 4 were constructed using the data set obtained for 40 to 140 particles under various magnifications. The average particle size (d_{avg}) for $NaBH_4$ and KNO_3 and the needle thickness for NH_4NO_3 with the monodispersity value (s/d_{avg}) were, respectively, 150 nm (0.20), 1.8 μm (0.21), and 48 nm (0.31). At the current (initial) step of the study, ultrafine powders have been prepared only for sodium borohydride.

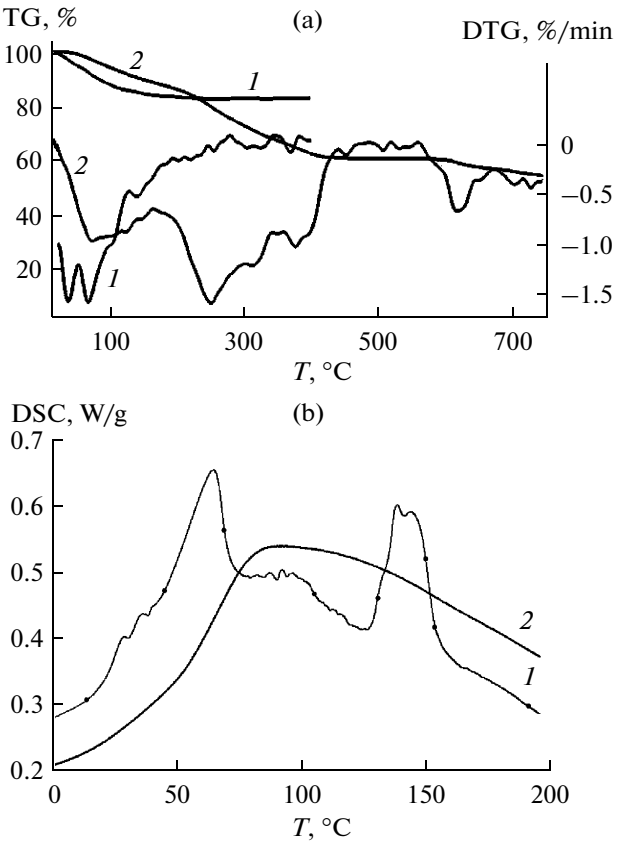

Fig. 8. (a) DTA and TG and (b) DSC data for $NaBH_4$ samples: (*1*) a reference and (*2*) a sample prepared by micellar synthesis.

X-ray powder diffraction showed that the samples were single phases and contained, respectively, KNO_3 (PDF no. 71-1558, space group *Pmcn*, $a = 5.4142$ Å, $b = 9.1659$ Å, $c = 6.4309$ Å) and NH_4NO_3 (PDF no. 47-867, space group *Pnmm*, $a = 4.9288$ Å, $b = 5.4408$ Å, $c = 5.7529$ Å; phase IV). Unlike the two preceding salts, the sodium borohydride powder was X-ray amorphous (Fig. 5).

The DSC and DTA endotherms correspond to phase transitions, polymorphic transitions, and decomposition of ammonium nitrate. Commercially available ammonium nitrate (the reference) experience polymorphic transitions (Fig. 6) in the vicinity of the following temperatures: −18°C (V → IV), −9°C (IV →III), 52°C (III → II), and 126.7°C (II → I). The phase transitions correspond to the melting of crystal water at 0°C, melting of ammonium nitrate at 169.1°C, and sublimation–decomposition of HA at 200°C < T < 300°C. The results obtained on the reference sample agree with the reported data.

In the sample prepared by micellar synthesis, there are no the first two low-temperature polymorphic transitions. This proves the absence of low-temperature polymorphs (phases V and IV), which make a lot of troubles in the use of ammonium nitrate. The melt-

ing temperature (166.8°C) was slightly lower than the reference value. A slightly unusual feature of the ultrafine powder was the appearance of a new phase transition (which is in addition a double one (see the inset in Fig. 6a), with peaks temperatures of approximately 41 and 44°C).

From thermoanalytical data, we may infer that the reference KNO_3 sample experiences a polymorphic transition at 132°C (phase II → phase I), melting at 333°C, and subsequent (at >400°C) decomposition consecutively to KNO_2 and K_2O. The behavior of the sample prepared by micellar synthesis is similar, but has some specific features, in particular, a greater weight loss, the polymorphic transition temperature increased to 149°C, the melting temperature decreased to 313°C, and broadened DTA peaks (Fig. 7).

Thermogravimetry (Fig. 8) shows that the thermal decomposition kinetics of the samples was almost identical to that of the references for NH_4NO_3 and KNO_3 and considerably different from the reference for $NaBH_4$. In the last case, the ultrafine powder had a great thermal stability up to 230°C; at higher temperatures, it decomposed with higher intensity than the reference (Fig. 8a).

In summary, this study has demonstrated the feasibility of preparing powders of water-soluble energy-intensive salts using oxyethylated surfactants and their microemulsions.

ACKNOWLEDGMENTS

This study was supported by the Russian Foundation for Basic Research (project no. 09-03-00511).

REFERENCES

1. W. Zhang, X. Qiao, and J. Chen, Colloids Surf. A: Physicochem. Eng. Asp. **299**, 22 (2007).
2. H. Huang, G. Q. Xu, W. Sh. Chin, et al., Nanotechnology **13**, 318 (2002).
3. P. Calandra, A. Longo, and L. V. Turco, J. Phys. Chem. B **107**, 25 (2003).
4. M. M. Husein, E. Rodil, and J. H. Vera, Langmuir **22**, 2264 (2006).
5. B. Viswanadh, S. Tikku, and K. C. Khilar, Colloid Surf. A: Physicochem. Eng. Asp. **208**, 149 (2007).
6. C. Giordano, A. Longo, L. V. Turco, and A. M. Venezia, Colloid Polym. Sci. **281**, 229 (2003).
7. V. Marciano, A. Minore, and L. V. Turco, Colloid Polym. Sci. **278**, 250 (2000).
8. I. Masalova and A. Ya. Malkin, Kolloidn. Zh. **69**, 206 (2007).
9. I. Masalova and A. Ya. Malkin, Kolloidn. Zh. **69**, 220 (2007).
10. L. V. Dubnov, N. S. Bakharevich, and A. I. Romanov, *Industrial Explosives* (Nedra, Moscow, 1988) [in Russian].
11. V. L. Baron and V. Kh. Kantor, *Engineering and Technology of Blasting in the USA* (Nedra, Moscow, 1989) [in Russian].
12. M. A. Cook, *The Science of Industrial Explosives* (IRECO Chemicals, Salt Lake City, 1974; Nedra, Moscow, 1974).
13. E. V. Zotov, *Electric Spark Initiation of Liquid Explosives*, Ed. by A. L. Mikhailov (Russian Federal Nuclear Center, Sarov) [in Russian].
14. S. R. Rafikov, S. A. Pavlova, and I. I. Tverdokhlebova, *Determination of Molecular Weights and Polydispersity for Macromolecular Compounds* (Izd–vo Akad. Nauk SSSR, Moscow, 1963) [in Russian].
15. P. J. Missel, N. A. Mazer, G. B. Benedek, and M. C. Carey, J. Phys. Chem. **87**, 1294 (1983).
16. A. V. Alekseev and S. A. Gromilov, Zh. Strukt. Khim. **51** (4), 772 (2010).
17. Powder Diffraction File: Inorganic Phases. Alphabetical Index (ICDD, 1995), p. 994
18. N. N. Mal'tseva and V. S. Khain, *Sodium Borohydride* (Nauka, Moscow, 1985).
19. A. I. Bulavchenko, E. K. Batishcheva, T. Yu. Podlipskaya, and V. G. Torgov, Kolloidn. Zh. **60**, 173 (1998).
20. A. I. Bulavchenko, E. K. Batishcheva, T. Yu. Podlipskaya, and V. G. Torgov, Kolloidn. Zh. **58**, 163 (1996).
21. P. Bonvicini, A. Levi, V. Lucchini, et al., J. Anal. Chem. Soc. **95**, 5960 (1973).
22. M. G. Demidova, A. I. Bulavchenko, and A. V. Alekseev, Russ. J. Inorg. Chem. **53**, 1446 (2008).
23. V. F. Volynets and M. P. Volynets, *The Analytical Chemistry of Nitrogen* (Nauka, Moscow, 1977) [in Russian].
24. H. Schott, A. E. Royce, and S. K. Han, J. Colloid Interface Sci. **98** (1), 196 (1984).
25. A. I. Bulavchenko, A. T. Arymbaeva, and V. V. Tatarchuk, Zh. Fiz. Khim. **82**, 920 (2008).
26. A. I. Bulavchenko, A. I. Tatarchuk, O. A. Bulavchenko, and A. T. Arymbaeva, Russ. J. Inorg. Chem. **50**, 786 (2005).